

Channel Shaping Using Reconfigurable Intelligent Surfaces: From Diagonal to Beyond

Yang Zhao, *Member, IEEE*, Hongyu Li, *Graduate Student Member, IEEE*,
Massimo Franceschetti, *Fellow, IEEE*, and Bruno Clerckx, *Fellow, IEEE*

Abstract—Reconfigurable Intelligent Surface (RIS) is a promising technology that recycles and redistributes ambient waves for improved wireless performance. This paper investigates the use of passive RIS for channel shaping in Multiple-Input Multiple-Output (MIMO) Point-to-point Channel (PC) and Interference Channel (IC). We depart from the widely-adapted diagonal phase shift model and focus on a general asymmetric Beyond-Diagonal (BD) architecture, which allows off-diagonal entries by in-group connections between elements. For arbitrary group size, we propose a closed-form iterative algorithm for quadratic problems and a Riemannian Conjugate Gradient (RCG) algorithm for general problems. Various case studies are then conducted, including rate maximization and Pareto singular value characterization for PC, and interference alignment and Weighted Sum-Rate (WSR) maximization for IC. To quantify channel shaping capability, we also derive analytical bounds under specific scenarios and validate those by aforementioned methods. Simulation results suggest the advantage of BD RIS scales with group size, while dyadic or tetradic architecture usually strikes a good balance between performance and complexity. Our findings unlock unprecedented efficiency and adaptability, paving the way for smarter and greener wireless environments.

Index Terms—Reconfigurable intelligent surface, channel shaping, point-to-point channel, interference channel.

I. INTRODUCTION

The quest for reliable, high-speed, and ubiquitous wireless connectivity has been long-standing since Marconi's illuminating radio in 1895. Great successes have been made at transmitter and receiver sides over the past century, and the society is unprecedentedly close to the Shannon limit [1]. Today we are witnessing a paradigm shift from *connectivity* to *intelligence*, where the wireless environment is no longer a chaotic medium but a conscious agent that serves on demand. This is made possible by the recent advances in Reconfigurable Intelligent Surface (RIS), a real-time programmable metasurface made of low-power reflecting elements. It can manipulate the amplitude, phase, frequency, and polarization of the scattered waves [2] with a higher energy efficiency, lower cost, lighter footprint, and greater scalability than conventional relays. Using RIS for *passive beamforming* has attracted significant interest in wireless communication, backscatter, sensing, and power transfer literature [3]–[13], reporting a second-order array gain and fourth-order power scaling law (with proper waveform). On the other hand, RIS also enables *backscatter modulation* by dynamically switching between different patterns, as investigated [14]–[20] and prototyped [21], [22]. Although fruitful outcomes have been harvested by fancy optimization tools, one fundamental yet critical unanswered question is the *channel shaping* capability of RIS: To what extent can RIS reshape the wireless channel?

Before answering the question, we first need to revisit the RIS architecture.

II. ASSUMPTION

We introduce Beyond-Diagonal (BD) RIS in Multiple-Input Multiple-Output (MIMO) Point-to-point Channel (PC) and Interference Channel (IC). All proposals are based on assumption of *asymmetric* passive BD RIS, i.e., symmetry constraint $\Theta_g = \Theta_g^T$ is relaxed. This is feasible when asymmetric passive components (e.g., ring hybrids and branch-line hybrids) [23] are available. This assumption was also made in Hongyu's papers [24], [25]. For quadratic problems, the proposed algorithms may be extended to symmetric BD RIS by replacing singular value decomposition with Takagi factorization [26].

III. MIMO-PC

A. Channel Power Maximization

Consider a BD RIS with N^S elements, which is divided into G groups of equal L elements.

$$\max_{\Theta} \left\| \mathbf{H}^D + \sum_g \mathbf{H}_g^B \Theta_g \mathbf{H}_g^F \right\|_F^2 \quad (1a)$$

$$\text{s.t.} \quad \Theta_g^H \Theta_g = \mathbf{I}, \quad \forall g \in \mathcal{G} \triangleq \{1, \dots, G\}. \quad (1b)$$

For *symmetric* BD-RIS, the problem has been solved in

- Matteo's paper [27]: SISO and equivalent¹;
- Ignacio's paper [28]: SISO and directless MISO/SIMO.

Remark 1. The difficulty of (1) is that the RIS needs to balance the additive (direct-indirect) and multiplicative (forward-backward) eigenspace alignment. Interestingly, it has the same form as the weighted orthogonal Procrustes problem [29]:

$$\min_{\Theta} \left\| \mathbf{C} - \mathbf{A} \Theta \mathbf{B} \right\|_F^2 \quad (2a)$$

$$\text{s.t.} \quad \Theta^H \Theta = \mathbf{I}. \quad (2b)$$

There exists no trivial solution to (2). One lossy transformation, by moving Θ to one side [30], formulates a standard orthogonal Procrustes problem:

$$\min_{\Theta} \left\| \mathbf{A}^\dagger \mathbf{C} - \Theta \mathbf{B} \right\|_F^2 \quad (3a)$$

$$\text{s.t.} \quad \Theta^H \Theta = \mathbf{I}. \quad (3b)$$

(3) has a global optimal solution $\Theta^* = \mathbf{U} \mathbf{V}^H$, where \mathbf{U} and \mathbf{V} are left and right singular matrix of $\mathbf{A}^\dagger \mathbf{C} \mathbf{B}^H$ [31].

¹Single-stream MIMO with given precoder and combiner.

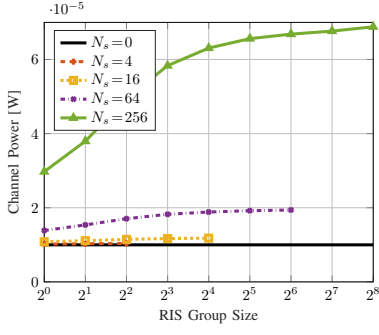


Fig. 1. Average channel power versus RIS elements N^S and group size L . $(N^T, N^R) = (8, 4)$, $(A^D, A^F, A^B) = (65, 54, 46)$ dB.

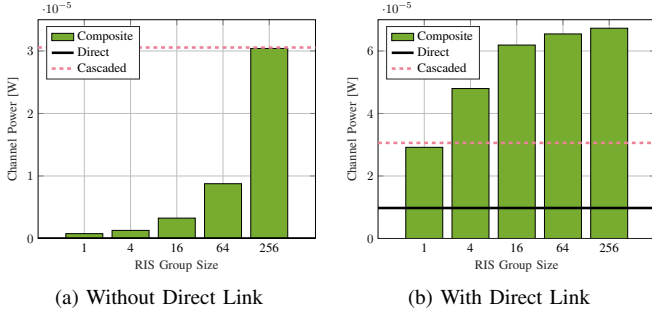


Fig. 2. Average channel power versus RIS group size L . $(N^T, N^S, N^R) = (8, 256, 4)$, $(A^D, A^F, A^B) = (65, 54, 46)$ dB.

This low-complexity solution will be compared with the one proposed later.

Inspired by [32], we propose an iterative algorithm to solve (1). The idea is to successively approximate the quadratic objective with a sequence of affine functions and solve the resulting subproblems in closed form.

Proposition 1. Start from any $\Theta^{(0)}$, the sequence

$$\Theta_g^{(r+1)} = \mathbf{U}_g^{(r)} \mathbf{V}_g^{(r)}, \quad \forall g \quad (4)$$

converges to a stationary point of (1), where $\mathbf{U}_g^{(r)}$ and $\mathbf{V}_g^{(r)}$ are left and right singular matrix of

$$\begin{aligned} \mathbf{M}_g^{(r)} = & \mathbf{H}_g^B \mathbf{H}_g^D \mathbf{H}_g^F \mathbf{H} + \sum_{g' < g} \mathbf{H}_{g'}^B \mathbf{H}_{g'}^H \mathbf{H}_{g'}^B \Theta_{g'}^{(r+1)} \mathbf{H}_{g'}^F \mathbf{H}_{g'}^H \\ & + \sum_{g' \geq g} \mathbf{H}_{g'}^B \mathbf{H}_{g'}^H \Theta_{g'}^{(r)} \mathbf{H}_{g'}^F \mathbf{H}_{g'}^H. \end{aligned} \quad (5)$$

Proof. To be added. \square

Fig. 1 shows that, apart from adding reflecting elements N^S , increasing the group size L also improves the channel power. This behavior is more pronounced for a large RIS. For example, the gain of pairwise connection is 2.8 % for $N^S = 16$ and 28 % for $N^S = 256$. It implies that the channel shaping capability of BD RIS scales with group size L .

Fig. 2b and 2a compare the average channel power without and with direct link. ‘‘Cascaded’’ means the sum of element-wise product of first $N = \min(N^T, N^S, N^R)$ eigenvalues (i.e., element-wise power product) of the forward and backward channels. We observe that diagonal RIS wastes substantial cascaded

power and struggles to align the direct-indirect eigenspace. When the direct link is absent, only 2.6 % of available power is utilized by diagonal RIS while 100 % power is recycled by fully-connected RIS. When the direct link is present, the proposed BD RIS design can balance the direct-indirect and forward-backward eigenspace alignment for an optimal channel boost. It is worth noting that, when L is sufficiently large, the composite channel power surpasses the power sum of direct and cascaded channels, thanks to the constructive *amplitude superposition* of direct and cascaded channels. This again emphasizes the advantage of in-group connection of BD RIS.

B. Rate Maximization

The problem is formulated w.r.t. precoder (instead of transmit covariance matrix) for reference:

$$\max_{\mathbf{W}, \Theta} \quad R = \log \det \left(\mathbf{I} + \frac{\mathbf{W}^H \mathbf{H}^H \mathbf{H} \mathbf{W}}{\eta} \right) \quad (6a)$$

$$\text{s.t.} \quad \|\mathbf{W}\|_F^2 \leq P, \quad (6b)$$

$$\Theta_g^H \Theta_g = \mathbf{I}, \quad \forall g. \quad (6c)$$

(6) is jointly non-convex and solved by Alternating Optimization (AO). For a given Θ , the optimal precoder is given by

$$\mathbf{W}^* = \mathbf{V} \mathbf{S}^{*1/2}, \quad (7)$$

where \mathbf{V} is right singular matrix of \mathbf{H} and \mathbf{S}^* is a diagonal matrix of the water-filling power allocation. For a given \mathbf{W} , we update Θ by Riemannian Conjugate Gradient (RCG) method along the geodesics [33].

Remark 2. A geodesic refers to the shortest path between two points in a Riemannian manifold. Unitary constraint (6c) translates to a Stiefel manifold where the geodesics have simple expressions described by the exponential map [34].

For general optimization problems with block unitary constraint, the adapted RCG method at iteration r for block g is summarized below, where $f(\Theta_g^{(r)})$ is the objective function also evaluated over $\{\{\Theta_{g'}^{(r+1)}\}_{g' < g}, \{\Theta_{g'}^{(r)}\}_{g' > g}\}$.

1) Compute the Euclidean gradient

$$\nabla_g^E(r) = \frac{\partial f(\Theta_g^{(r)})}{\partial \Theta_g^*}; \quad (8)$$

2) Translate to the Riemannian gradient

$$\nabla_g^R(r) = \nabla_g^E(r) \Theta_g^{(r)H} - \Theta_g^{(r)} \nabla_g^E(r)^H; \quad (9)$$

3) Determine the weight factor

$$\gamma_g^{(r)} = \frac{\text{tr}((\nabla_g^R(r) - \nabla_g^R(r-1)) \nabla_g^R(r)^H)}{\text{tr}(\nabla_g^R(r-1) \nabla_g^R(r-1)^H)}; \quad (10)$$

4) Compute the conjugate direction

$$\mathbf{D}_g^{(r)} = \nabla_g^R(r) + \gamma_g^{(r)} \mathbf{D}_g^{(r-1)}; \quad (11)$$

Algorithm 1: RCG Method for RIS MIMO-PC Rate Maximization
Input: $\mathbf{H}^D, \mathbf{H}^F, \mathbf{H}^B, \mathbf{W}, L, \eta$
Output: Θ^*

```

1:  $r \leftarrow 0, \Theta^{(0)}$ 
2: Repeat
3:    $r \leftarrow r + 1$ 
4:   For  $g \leftarrow 1$  to  $G$ 
5:      $\Theta_g^{(r)} \leftarrow (14), (9)-(13)$ 
6:   End For
7: Until  $|R^{(r)} - R^{(r-1)}|/R^{(r-1)} \leq \epsilon$ 

```

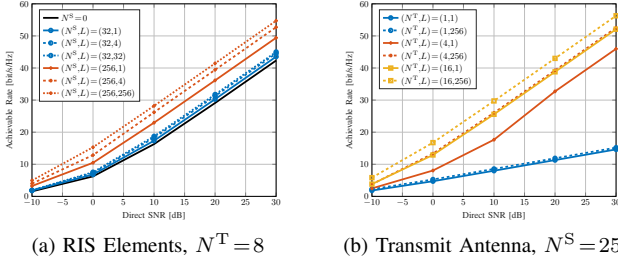


Fig. 3. Average achievable rate versus group size L . $N^R = 4$, $(A^D, A^F, A^B) = (65, 54, 46)$ dB.

5) Determine the Armijo step size²

$$\mu_g^{(r)} = \arg\max_{\mu_g} f\left(\exp(\mu_g \mathbf{D}_g^{(r)}) \Theta_g^{(r)}\right); \quad (12)$$

6) Perform rotational update along local geodesics

$$\Theta_g^{(r+1)} = \exp\left(\mu_g^{(r)} \mathbf{D}_g^{(r)}\right) \Theta_g^{(r)}. \quad (13)$$

Remark 3. The adapted RCG method leverages the fact that block unitary matrices are closed under multiplication (but not necessarily under addition). Its advantage over universal manifold optimization [35], [36] is trifold:

- No retraction is involved;
- Lower computational complexity per iteration [34];
- Faster convergence thanks appropriate operational space.

The complex derivative of (6a) w.r.t. RIS block g is

$$\frac{\partial R}{\partial \Theta_g^*} = \frac{1}{\eta} \mathbf{H}_g^B \mathbf{H}^B \mathbf{H}^W \left(\mathbf{I} + \frac{\mathbf{W}^H \mathbf{H}^H \mathbf{H}^W}{\eta} \right)^{-1} \mathbf{W}^H \mathbf{H}_g^F. \quad (14)$$

Algorithm 1 summarizes the adapted RCG method for the RIS rate maximization subproblem.

Fig. 3a illustrates how RIS configuration influences the MIMO PC achievable rate. To ensure a 20 bit/s/Hz transmission, an Signal-to-Noise Ratio (SNR) of 13.5 dB is required for a 8T4R system. This value decreases to 12.5 dB (resp. 8 dB) when 32- (resp. 256-) element diagonal RIS is present. If tetrads can be formed in BD RIS, the SNR can be reduced by another 20% (resp. 44%). Further increase in L yields a marginal gain and incurs $\mathcal{O}(L^2)$ connections. We thus conclude dyadic or tetradic BD RIS usually strike a good balance between performance and complexity.

²To double the step size, simply square the argument instead of recomputing the matrix exponential, i.e., $\exp(2\mu_g \mathbf{D}_g) = \exp^2(\mu_g \mathbf{D}_g)$.

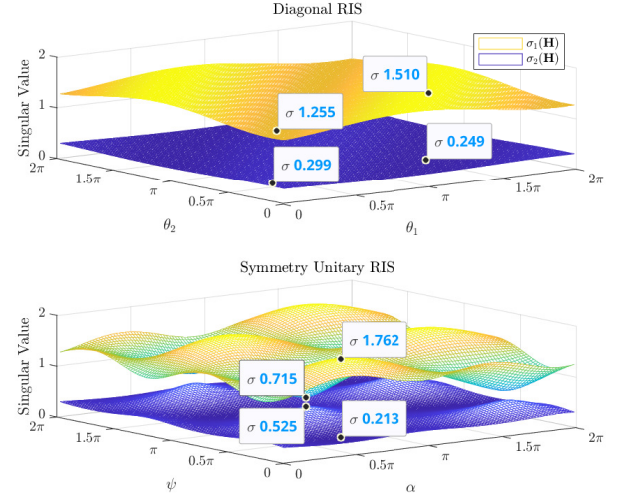


Fig. 4. Channel singular value shaping by diagonal and symmetry unitary RIS. $(N^T, N^S, N^R) = (2, 2, 2)$. Direct link is absent.

C. Channel Singular Value Redistribution

We first show the channel shaping benefit of BD RIS by a toy example. Consider $(N^T, N^S, N^R) = (2, 2, 2)$ and assume the direct link is absent. The diagonal RIS is $\Theta^D = \text{diag}(e^{j\theta_1}, e^{j\theta_2})$ while the unitary RIS has 4 independent angular parameters

$$\Theta^U = e^{j\phi} \begin{bmatrix} e^{j\alpha} \cos\psi & e^{j\beta} \sin\psi \\ -e^{-j\beta} \sin\psi & e^{-j\alpha} \cos\psi \end{bmatrix}. \quad (15)$$

When the direct link is absent, ϕ has no impact on the singular value because $\text{sv}(e^{j\phi} \mathbf{A}) = \text{sv}(\mathbf{A})$. For a fair comparison, we enforce symmetry with $\beta = \pi/2$. Fig. 4 illustrates all possible channel singular values achieved by diagonal and symmetry unitary RIS. Despite using the same number of elements and parameters, BD RIS provides much wider dynamic ranges of $\sigma_1(\mathbf{H})$ and $\sigma_2(\mathbf{H})$ than diagonal RIS. Larger gaps are expected when the symmetry constraint can be relaxed.

We then analyze the channel shaping capability of BD RIS under specific setups.

1) *Rank-Deficient Channel:* In rank-deficient channels, BD RIS Θ^B cannot achieve a higher Degree of Freedom (DoF) than diagonal RIS Θ^D . This is because $\text{sv}(\Theta^B) = \text{sv}(\Theta^D) = \mathbf{1}$ and

$$\begin{aligned} \text{rank}(\mathbf{H}) &\leq \text{rank}(\mathbf{H}^D) + \text{rank}(\mathbf{H}^B \Theta \mathbf{H}^F) \\ &\leq \text{rank}(\mathbf{H}^D) + \min(\text{rank}(\mathbf{H}^B), \text{rank}(\Theta), \text{rank}(\mathbf{H}^F)). \end{aligned} \quad (16)$$

Note BD RIS can still provide a higher indirect SNR as shown in Fig. 1 and 2.

2) *Rank-1 Indirect Channel:* The indirect channel is rank-1 iff the forward or backward channel is rank-1. Let $\mathbf{H}^F = \sigma^F \mathbf{u}^F \mathbf{v}^{F^H}$ without loss of generality. In this case, the channel Gram matrix can be written as Hermitian-plus-rank-1:

$$\mathbf{G} \triangleq \mathbf{H} \mathbf{H}^H = \mathbf{Y} + \mathbf{z} \mathbf{z}^H, \quad (17)$$

where $\mathbf{Y} \triangleq \mathbf{H}^D(\mathbf{I} - \mathbf{v}^F \mathbf{v}^{F^H})\mathbf{H}^D = \mathbf{T}\mathbf{T}^H$ and $\mathbf{z} \triangleq \sigma^F \mathbf{H}^B \mathbf{\Theta} \mathbf{u}^F + \mathbf{H}^D \mathbf{v}^F$. Regardless of RIS size and structure³, its n -th ($n \geq 2$) eigenvalues are bounded by the Cauchy interlacing formula [31]

$$\lambda_1(\mathbf{Y}) \geq \lambda_2(\mathbf{G}) \geq \lambda_2(\mathbf{Y}) \geq \dots \geq \lambda_{N-1}(\mathbf{Y}) \geq \lambda_N(\mathbf{G}) \geq \lambda_N(\mathbf{Y}). \quad (18)$$

The equivalent singular value inequality is

$$\sigma_1(\mathbf{T}) \geq \sigma_2(\mathbf{H}) \geq \sigma_2(\mathbf{T}) \geq \dots \geq \sigma_{N-1}(\mathbf{T}) \geq \sigma_N(\mathbf{H}) \geq \sigma_N(\mathbf{T}). \quad (19)$$

(19) implies that, if the indirect channel is rank-1, then the RIS can at most enlarge the n -th ($n \geq 2$) channel singular value to the $(n-1)$ -th singular value of \mathbf{T} . Note that the largest channel singular value is unbounded with a sufficiently large RIS.

3) *Fully-Connected RIS Without Direct Link*: Denote the singular value decomposition of forward / backward channels as $\mathbf{H}^{B/F} = \mathbf{U}^{B/F} \mathbf{\Sigma}^{B/F} \mathbf{V}^{B/F^H}$. The composite channel is

$$\mathbf{H} = \mathbf{H}^B \mathbf{\Theta} \mathbf{H}^F = \mathbf{U}^B \mathbf{\Sigma}^B \mathbf{X} \mathbf{\Sigma}^F \mathbf{V}^{F^H}, \quad (20)$$

where $\mathbf{X} = \mathbf{V}^{B^H} \mathbf{\Theta} \mathbf{U}^F$.

Proposition 2. *In this case, the singular value bounds on \mathbf{H} are equivalent to the singular value bounds on \mathbf{BF} , where \mathbf{B} and \mathbf{F} are arbitrary matrices with singular values $\mathbf{\Sigma}^B$ and $\mathbf{\Sigma}^F$.*

Proof. We first observe that singular value control problem can be solved w.r.t. unitary \mathbf{X} and retrieved by $\mathbf{\Theta} = \mathbf{V}^B \mathbf{X} \mathbf{U}^{F^H}$. Also, $\text{sv}(\mathbf{U}^B \mathbf{\Sigma}^B \mathbf{X} \mathbf{\Sigma}^F \mathbf{V}^{F^H}) = \text{sv}(\bar{\mathbf{U}}^B \mathbf{\Sigma}^B \bar{\mathbf{V}}^{B^H} \bar{\mathbf{U}}^F \mathbf{\Sigma}^F \bar{\mathbf{V}}^{F^H}) = \text{sv}(\mathbf{BF})$ where $\bar{\mathbf{U}}^{B/F}$ and $\bar{\mathbf{V}}^{B/F}$ are arbitrary unitary matrices. \square

The problem now becomes, given $\mathbf{\Sigma}^B$ and $\mathbf{\Sigma}^F$, what can we say about the singular value of \mathbf{BF} . One comprehensive answer is Horn's inequality [38]: for all admissible triples (I, J, K) ,

$$\prod_{k \in K} \sigma_k(\mathbf{BF}) \leq \prod_{i \in I} \sigma_i(\mathbf{B}) \prod_{j \in J} \sigma_j(\mathbf{F}). \quad (21)$$

It gives upper bound on the largest singular value and lower bound on the smallest singular value:

$$\sigma_1(\mathbf{BF}) \leq \sigma_1(\mathbf{B}) \sigma_1(\mathbf{F}) \quad (22)$$

$$\sigma_N(\mathbf{BF}) \geq \sigma_N(\mathbf{B}) \sigma_N(\mathbf{F}). \quad (23)$$

Another useful result is introduced in [39]: for all $p > 0$,

$$\sum_n \sigma_n^p(\mathbf{BF}) \leq \sum_n \sigma_n^p(\mathbf{B}) \sigma_n^p(\mathbf{F}). \quad (24)$$

When $p=2$, it implies the channel energy is upper bounded by the sum of element-wise power product of the forward and backward channels, as illustrated in Fig. 2(a). Interestingly, (22)–(24) are simultaneously tight when $\mathbf{X} = \mathbf{I}$ and $\mathbf{\Theta} = \mathbf{V}^B \mathbf{U}^{F^H}$. This solution was claimed in [40] to achieve channel capacity, but it is not true at moderate SNR.

Finally, we characterize the *Pareto front* of channel singular values via optimization approach.

³A similar conclusion was made for diagonal RIS in [37].

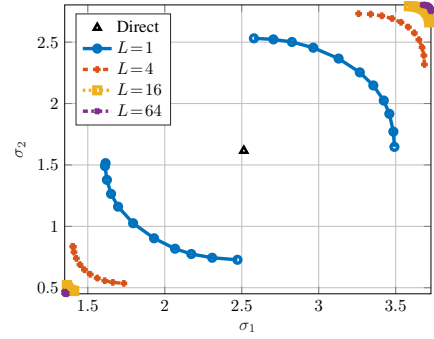


Fig. 5. Singular value Pareto front. $(N^T, N^S, N^R) = (4, 64, 2)$, $(\Lambda^D, \Lambda^F, \Lambda^B) = (0, -17.5, -17.5)$ dB.

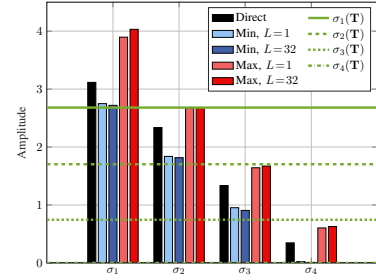


Fig. 6. Singular value bounds for rank-1 indirect channel. $(N^T, N^S, N^R) = (4, 32, 4)$, $(\Lambda^D, \Lambda^F, \Lambda^B) = (0, -17.5, -17.5)$ dB.

$$\max_{\mathbf{\Theta}} / \min_{\mathbf{\Theta}} J_1 = \sum_n \rho_n \sigma_n(\mathbf{H}) \quad (25a)$$

$$\text{s.t.} \quad \mathbf{\Theta}_g^H \mathbf{\Theta}_g = \mathbf{I}, \quad \forall g, \quad (25b)$$

where ρ_n is the weight of n -th singular value. The complex derivative of (25a) w.r.t. RIS block g is

$$\frac{\partial J_1}{\partial \mathbf{\Theta}_g^*} = \mathbf{H}_g^B \mathbf{H}_g^H \mathbf{U} \text{diag}(\boldsymbol{\rho}) \mathbf{V}^H \mathbf{H}_g^{F^H}, \quad (26)$$

where \mathbf{U} and \mathbf{V} are left and right singular matrix of \mathbf{H} . (25) can be solved by RCG Algorithm 1 with (14) replaced by (26).

The Pareto front and evolving trend of channel singular values are shown in Fig. 5 and 6. Clearly, BD RIS with a larger group size can redistribute the channel singular values to a wider range.

IV. MIMO-IC

A. Leakage Interference Minimization

$$\min_{\mathbf{\Theta}, \{\mathbf{G}_k\}, \{\mathbf{W}_k\}} \sum_{j \neq k} \|\mathbf{G}_k (\mathbf{H}_{kj}^D + \mathbf{H}_k^B \mathbf{\Theta} \mathbf{H}_j^F) \mathbf{W}_j\|_F^2 \quad (27a)$$

$$\text{s.t.} \quad \mathbf{\Theta}_g^H \mathbf{\Theta}_g = \mathbf{I}, \quad \forall g, \quad (27b)$$

$$\mathbf{G}_k \mathbf{G}_k^H = \mathbf{I}, \quad \mathbf{W}_k^H \mathbf{W}_k = \mathbf{I}, \quad \forall k. \quad (27c)$$

The non-convex problem can be solved by Block Coordinate Descent (BCD) method. For a given $\mathbf{\Theta}$, it reduces to conventional linear beamforming problem, for which an iterative algorithm

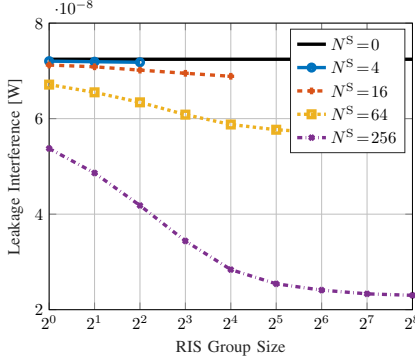


Fig. 7. Average leakage interference versus RIS elements N^S and group size L . Transmitters and receivers are randomly generated in a disk of radius 50 m centered at the RIS. $(N^T, N^R, N^E, K) = (8, 4, 3, 5)$, $(\gamma^D, \gamma^F, \gamma^B) = (3, 2, 4, 2, 4)$, and reference pathloss at 1 m is -30 dB.

alternating between the original and reciprocal networks is proposed in [41], [42]. At iteration r , the combiner at receiver k is updated as

$$\mathbf{G}_k^{(r)} = \mathbf{U}_{k,N}^{(r-1)H}, \quad (28)$$

where $\mathbf{U}_{k,N}^{(r-1)}$ is the eigenvectors corresponding to N smallest eigenvalues of interference covariance matrix $\mathbf{Q}_k^{(r-1)} = \sum_{j \neq k} \mathbf{H}_{kj} \mathbf{W}_j^{(r-1)} \mathbf{W}_j^{(r-1)H} \mathbf{H}_{kj}^H$. The precoder at transmitter j is updated as

$$\mathbf{W}_j^{(r)} = \bar{\mathbf{U}}_{j,N}^{(r)}, \quad (29)$$

where $\bar{\mathbf{U}}_{j,N}^{(r)}$ corresponds to interference covariance matrix $\bar{\mathbf{Q}}_j^{(r)} = \sum_{k \neq j} \mathbf{H}_{kj}^H \mathbf{G}_k^{(r)} \mathbf{G}_k^{(r)H} \mathbf{H}_{kj}$ in the reciprocal network. Once $\{\mathbf{G}_k\}$ and $\{\mathbf{W}_k\}$ are determined, we define $\bar{\mathbf{H}}_{kj}^D \triangleq \mathbf{G}_k \mathbf{H}_{kj}^D \mathbf{W}_j$, $\bar{\mathbf{H}}_k^B \triangleq \mathbf{G}_k \mathbf{H}_k^B$, and $\bar{\mathbf{H}}_j^F \triangleq \mathbf{H}_j^F \mathbf{W}_j$. The BD RIS subproblem reduces to

$$\min_{\Theta} \sum_{j \neq k} \|(\bar{\mathbf{H}}_{kj}^D + \bar{\mathbf{H}}_k^B \Theta \bar{\mathbf{H}}_j^F)\|_F^2 \quad (30a)$$

$$\text{s.t. } \Theta_g^H \Theta_g = \mathbf{I}, \quad \forall g. \quad (30b)$$

Proposition 3. Start from any $\Theta^{(0)}$, the sequence

$$\Theta_g^{(r+1)} = \mathbf{U}_g^{(r)} \mathbf{V}_g^{(r)}, \quad \forall g \quad (31)$$

converges to a stationary point of (30), where $\mathbf{U}_g^{(r)}$ and $\mathbf{V}_g^{(r)}$ are left and right singular matrix of

$$\mathbf{M}_g^{(r)} = \sum_{j \neq k} (\mathbf{B}_{k,g} \Theta_g^{(r)} \mathbf{H}_{j,g}^F - \mathbf{H}_{k,g}^B \mathbf{D}_{k,j,g}^{(r)}) \mathbf{H}_{j,g}^F{}^H, \quad (32)$$

where $\mathbf{B}_{k,g} = \lambda_1(\mathbf{H}_{k,g}^B \mathbf{H}_{k,g}^B{}^H) \mathbf{I} - \mathbf{H}_{k,g}^B \mathbf{H}_{k,g}^B$ and

$$\mathbf{D}_{k,j,g}^{(r)} = \mathbf{H}_{jk}^D + \sum_{g' < g} \mathbf{H}_{k,g'}^B \mathbf{H}_{g'}^{(r+1)} \mathbf{H}_{k,g'}^F + \sum_{g' > g} \mathbf{H}_{k,g'}^B \mathbf{H}_{g'}^{(r)} \mathbf{H}_{k,g'}^F. \quad (33)$$

Proof. To be added. \square

Fig. 7 illustrates how BD RIS helps to reduce the leakage interference. In this case, a fully-connected 2^n -element BD RIS is almost as good as a diagonal 2^{n+2} -element RIS in terms of leakage interference. Interestingly, the result suggests that BD

RIS can achieve a higher DoF than diagonal RIS in MIMO-IC, which is not the case in MIMO-PC (as discussed in III-C1).

B. Weighted Sum-Rate Maximization

$$\max_{\Theta, \{\mathbf{W}_k\}} J_2 = \sum_k \rho_k \log \det \left(\mathbf{I} + \mathbf{W}_k \mathbf{H}_{kj}^H \mathbf{Q}_k^{-1} \mathbf{H}_{kj} \mathbf{W}_k \right) \quad (34a)$$

$$\text{s.t. } \Theta_g^H \Theta_g = \mathbf{I}, \quad \forall g, \quad (34b)$$

$$\|\mathbf{W}_k\|_F^2 \leq P_k, \quad \forall k \quad (34c)$$

where ρ_k is the weight of user k and \mathbf{Q}_k is the interference-plus-noise covariance matrix

$$\mathbf{Q}_k = \sum_{j \neq k} \mathbf{H}_{kj} \mathbf{W}_j \mathbf{W}_j^H \mathbf{H}_{kj}^H + \eta \mathbf{I}. \quad (35)$$

For a given Θ , (34) reduces to conventional linear beamforming problem, for which a closed-form iterative solution based on Weighted Sum-Rate (WSR)-Weighted MMSE (WMMSE) relationship is proposed in [43]. At iteration r , the Minimum Mean-Square Error (MMSE) combiner at receiver k is

$$\mathbf{G}_k^{(r)} = \mathbf{W}_k^{(r-1)H} \mathbf{H}_{kk}^H (\mathbf{Q}_k^{(r-1)} + \mathbf{H}_{kk} \mathbf{W}_k^{(r-1)} \mathbf{W}_k^{(r-1)H} \mathbf{H}_{kk}^H)^{-1}, \quad (36)$$

the corresponding error matrix is

$$\mathbf{E}_k^{(r)} = (\mathbf{I} + \mathbf{W}_k^{(r-1)H} \mathbf{H}_{kk}^H \mathbf{Q}_k^{(r-1)} \mathbf{H}_{kk} \mathbf{W}_k^{(r-1)})^{-1}, \quad (37)$$

the Mean-Square Error (MSE) weight is

$$\Omega_k^{(r)} = \rho_k \mathbf{E}_k^{(r)-1}, \quad (38)$$

the Lagrange multiplier is

$$\lambda_k^{(r)} = \frac{\text{tr}(\eta \Omega_k^{(r)} \mathbf{G}_k^{(r)} \mathbf{G}_k^{(r)H} + \sum_j \Omega_k^{(r)} \mathbf{T}_{kj}^{(r)} \mathbf{T}_{kj}^{(r)H} - \Omega_j^{(r)} \mathbf{T}_{jk}^{(r)} \mathbf{T}_{jk}^{(r)H})}{P_k}, \quad (39)$$

where $\mathbf{T}_{kj}^{(r)} = \mathbf{G}_k^{(r)} \mathbf{H}_{kj} \mathbf{W}_j^{(r)}$. The precoder at transmitter k is

$$\mathbf{W}_k^{(r)} = \left(\sum_j \mathbf{H}_{jk}^H \mathbf{G}_j^{(r)} \Omega_k^{(r)} \mathbf{G}_j^{(r)} \mathbf{H}_{jk} + \lambda_k^{(r)} \mathbf{I} \right)^{-1} \mathbf{H}_{kk}^H \mathbf{G}_j^{(r)} \Omega_k^{(r)}. \quad (40)$$

Once $\{\mathbf{W}_k\}$ is determined, the complex derivative of (34a) w.r.t. RIS block g is

$$\begin{aligned} \frac{\partial J_2}{\partial \Theta_g^*} &= \sum_k \rho_k \mathbf{H}_{k,g}^B \mathbf{H}_{k,g}^B{}^H \mathbf{Q}_k^{-1} \mathbf{H}_{kk} \mathbf{W}_k \mathbf{E}_k \mathbf{W}_k^H \\ &\quad \times (\mathbf{H}_{k,g}^F{}^H - \mathbf{H}_{kk}^H \mathbf{Q}_k^{-1} \sum_{j \neq k} \mathbf{H}_{kj} \mathbf{W}_j \mathbf{W}_j^H \mathbf{H}_{j,g}^F). \end{aligned} \quad (41)$$

The RIS subproblem can be solved by RCG Algorithm 1 with (14) replaced by (41).

A new observation from Fig. 8 that the interference alignment capability of BD RIS scales much faster with group size than number of elements.⁴

⁴The results are not very stable and depend heavily on initialization.

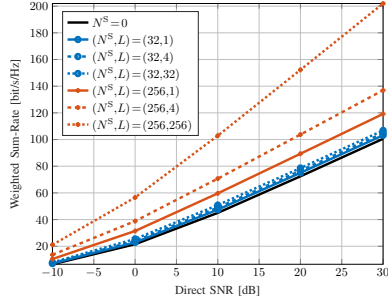


Fig. 8. Average weighted sum-rate versus SNR, RIS elements N^S and group size L . $(N^T, N^R, N^E, K) = (8, 4, 3, 5)$, $(A^D, A^F, A^B) = (65, 54, 46)$ dB, $\rho_k = 1$, $\forall k$.

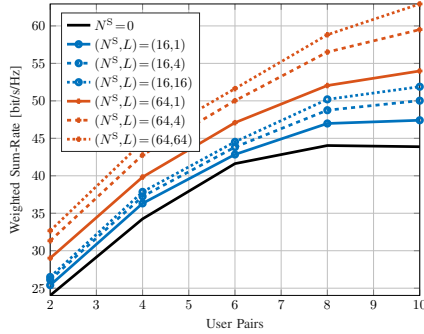


Fig. 9. Average weighted sum-rate versus user pairs K , RIS elements N^S and group size L at SNR=15dB. $(N^T, N^R, N^E) = (4, 4, 3)$, $\rho_k = 1$, $\forall k$.

REFERENCES

- [1] C. E. Shannon, "A mathematical theory of communication," *Bell System Technical Journal*, vol. 27, pp. 379–423, 7 1948. [Online]. Available: <https://ieeexplore.ieee.org/document/6773024>
- [2] E. Basar, M. D. Renzo, J. D. Rosny, M. Debbah, M.-S. Alouini, and R. Zhang, "Wireless communications through reconfigurable intelligent surfaces," *IEEE Access*, vol. 7, pp. 116 753–116 773, 2019. [Online]. Available: <https://ieeexplore.ieee.org/document/8796365/>
- [3] Q. Wu and R. Zhang, "Intelligent reflecting surface enhanced wireless network via joint active and passive beamforming," *IEEE Transactions on Wireless Communications*, vol. 18, pp. 5394–5409, 11 2019. [Online]. Available: <https://ieeexplore.ieee.org/document/8811733/>
- [4] —, "Beamforming optimization for wireless network aided by intelligent reflecting surface with discrete phase shifts," *IEEE Transactions on Communications*, vol. 68, pp. 1838–1851, 3 2020. [Online]. Available: <https://ieeexplore.ieee.org/document/8930608/>
- [5] Y. Yang, S. Zhang, and R. Zhang, "Irs-enhanced ofdma: Joint resource allocation and passive beamforming optimization," *IEEE Wireless Communications Letters*, vol. 9, pp. 760–764, 6 2020. [Online]. Available: <https://ieeexplore.ieee.org/document/8964457/>
- [6] B. Zheng, C. You, and R. Zhang, "Double-irs assisted multi-user mimo: Cooperative passive beamforming design," *IEEE Transactions on Wireless Communications*, vol. 20, pp. 4513–4526, 7 2021. [Online]. Available: <https://ieeexplore.ieee.org/document/9362274/>
- [7] X. Jia, J. Zhao, X. Zhou, and D. Niyato, "Intelligent reflecting surface-aided backscatter communications," vol. 2020-Janua. IEEE, 12 2020, pp. 1–6. [Online]. Available: <https://ieeexplore.ieee.org/document/9348003/>
- [8] Y. C. Liang, Q. Zhang, J. Wang, R. Long, H. Zhou, and G. Yang, "Backscatter communication assisted by reconfigurable intelligent surfaces," *Proceedings of the IEEE*, 2022.
- [9] R. Liu, M. Li, Y. Liu, Q. Wu, and Q. Liu, "Joint transmit waveform and passive beamforming design for ris-aided dfrc systems," *IEEE Journal of Selected Topics in Signal Processing*, pp. 1–1, 5 2022.
- [10] M. Hua, Q. Wu, C. He, S. Ma, and W. Chen, "Joint active and passive beamforming design for irs-aided radar-communication," *IEEE Transactions on Wireless Communications*, vol. 22, pp. 2278–2294, 4 2023.
- [11] Q. Wu, X. Zhou, W. Chen, J. Li, and X. Zhang, "Irs-aided wpns: A new optimization framework for dynamic irs beamforming," *IEEE Transactions on Wireless Communications*, pp. 1–1, 12 2021.
- [12] Z. Feng, B. Clerckx, and Y. Zhao, "Waveform and beamforming design for intelligent reflecting surface aided wireless power transfer: Single-user and multi-user solutions," *IEEE Transactions on Wireless Communications*, 2022.
- [13] Y. Zhao, B. Clerckx, and Z. Feng, "Irs-aided swipt: Joint waveform, active and passive beamforming design under nonlinear harvester model," *IEEE Transactions on Communications*, vol. 70, pp. 1345–1359, 2022.
- [14] R. Liu, H. Li, M. Li, and Q. Liu, "Symbol-level precoding design for intelligent reflecting surface assisted multi-user mimo systems." IEEE, 10 2019, pp. 1–6. [Online]. Available: <https://ieeexplore.ieee.org/document/9174065/>
- [15] R. Karasik, O. Simeone, M. D. Renzo, and S. S. Shitz, "Beyond max-snr: Joint encoding for reconfigurable intelligent surfaces," vol. 2020-June. IEEE, 6 2020, pp. 2965–2970. [Online]. Available: <https://ieeexplore.ieee.org/document/9174060/>
- [16] E. Basar, "Reconfigurable intelligent surface-based index modulation: A new beyond mimo paradigm for 6g," *IEEE Transactions on Communications*, vol. 68, pp. 3187–3196, 5 2020. [Online]. Available: <https://ieeexplore.ieee.org/document/8981888/>
- [17] T. Ma, Y. Xiao, X. Lei, P. Yang, X. Lei, and O. A. Dobre, "Large intelligent surface assisted wireless communications with spatial modulation and antenna selection," *IEEE Journal on Selected Areas in Communications*, vol. 38, pp. 2562–2574, 11 2020. [Online]. Available: <https://ieeexplore.ieee.org/document/9133588/>
- [18] Q. Zhang, Y.-C. Liang, and H. V. Poor, "Reconfigurable intelligent surface assisted mimo symbiotic radio networks," *IEEE Transactions on Communications*, vol. 69, pp. 4832–4846, 7 2021. [Online]. Available: <https://ieeexplore.ieee.org/document/9391685/>
- [19] M. Hua, Q. Wu, L. Yang, R. Schober, and H. V. Poor, "A novel wireless communication paradigm for intelligent reflecting surface based symbiotic radio systems," *IEEE Transactions on Signal Processing*, vol. 70, pp. 550–565, 4 2022. [Online]. Available: <http://arxiv.org/abs/2104.09161https://ieeexplore.ieee.org/document/9652042/>
- [20] Y. Zhao and B. Clerckx, "Riscatter: Unifying backscatter communication and reconfigurable intelligent surface," 12 2022. [Online]. Available: <http://arxiv.org/abs/2212.09121>
- [21] W. Tang, J. Y. Dai, M. Chen, X. Li, Q. Cheng, S. Jin, K. Wong, and T. J. Cui, "Programmable metasurface-based rf chain-free 8psk wireless transmitter," *Electronics Letters*, vol. 55, pp. 417–420, 4 2019. [Online]. Available: <https://onlinelibrary.wiley.com/doi/10.1049/el.2019.0400>
- [22] J. Y. Dai, W. Tang, L. X. Yang, X. Li, M. Z. Chen, J. C. Ke, Q. Cheng, S. Jin, and T. J. Cui, "Realization of multi-modulation schemes for wireless communication by time-domain digital coding metasurface," *IEEE Transactions on Antennas and Propagation*, vol. 68, pp. 1618–1627, 3 2020. [Online]. Available: <https://ieeexplore.ieee.org/document/8901437/>
- [23] H.-R. Ahn, *Asymmetric Passive Components in Microwave Integrated Circuits*. Wiley, 2006. [Online]. Available: <https://books.google.co.uk/books?id=X6WdLbOuSNQC>
- [24] H. Li, S. Shen, and B. Clerckx, "Beyond diagonal reconfigurable intelligent surfaces: From transmitting and reflecting modes to single-, group-, and fully-connected architectures," *IEEE Transactions on Wireless Communications*, vol. 22, pp. 2311–2324, 4 2023.
- [25] —, "Beyond diagonal reconfigurable intelligent surfaces: A multi-sector mode enabling highly directional full-space wireless coverage," *IEEE Journal on Selected Areas in Communications*, vol. 41, pp. 2446–2460, 8 2023.
- [26] R. A. Horn and C. R. Johnson, *Matrix Analysis*. Cambridge University Press, 2012. [Online]. Available: <https://books.google.co.uk/books?id=O7sgAwAAQBAJ>
- [27] M. Nerini, S. Shen, and B. Clerckx, "Closed-form global optimization of beyond diagonal reconfigurable intelligent surfaces," *IEEE Transactions on Wireless Communications*, pp. 1–1, 2023. [Online]. Available: <https://ieeexplore.ieee.org/document/10155675/>
- [28] I. Santamaria, M. Soleymani, E. Jorswieck, and J. Gutiérrez, "Snr maximization in beyond diagonal ris-assisted single and multiple antenna links," *IEEE Signal Processing Letters*, vol. 30, pp. 923–926, 2023. [Online]. Available: <https://ieeexplore.ieee.org/document/10187688/>
- [29] J. C. Gower and G. B. Dijkstra, *Procrustes Problems*. OUP Oxford, 2004. [Online]. Available: <https://books.google.co.uk/books?id=kRRREAAQBAJ>
- [30] T. Bell, "Global positioning system-based attitude determination and the orthogonal procrustes problem," *Journal of Guidance, Control, and Dynamics*, vol. 26, pp. 820–822, 9 2003. [Online]. Available: <https://arc.aiaa.org/doi/10.2514/2.5117>

- [31] G. H. Golub and C. F. V. Loan, *Matrix Computations*. Johns Hopkins University Press, 2013. [Online]. Available: <https://jhupbooks.press.jhu.edu/title/matrix-computations>
- [32] F. Nie, R. Zhang, and X. Li, "A generalized power iteration method for solving quadratic problem on the stiefel manifold," *Science China Information Sciences*, vol. 60, p. 112101, 11 2017. [Online]. Available: <http://link.springer.com/10.1007/s11432-016-9021-9>
- [33] T. Abrudan, J. Eriksson, and V. Koivunen, "Conjugate gradient algorithm for optimization under unitary matrix constraint," *Signal Processing*, vol. 89, pp. 1704–1714, 9 2009. [Online]. Available: <https://linkinghub.elsevier.com/retrieve/pii/S0165168409000814>
- [34] T. E. Abrudan, J. Eriksson, and V. Koivunen, "Steepest descent algorithms for optimization under unitary matrix constraint," *IEEE Transactions on Signal Processing*, vol. 56, pp. 1134–1147, 3 2008. [Online]. Available: <http://ieeexplore.ieee.org/document/4436033/>
- [35] P.-A. Absil, R. Mahony, and R. Sepulchre, *Optimization Algorithms on Matrix Manifolds*. Princeton University Press, 2009. [Online]. Available: <https://books.google.co.uk/books?id=NSQGQeLN3NcC>
- [36] C. Pan, G. Zhou, K. Zhi, S. Hong, T. Wu, Y. Pan, H. Ren, M. D. Renzo, A. L. Swindlehurst, R. Zhang, and A. Y. Zhang, "An overview of signal processing techniques for ris/firs-aided wireless systems," *IEEE Journal of Selected Topics in Signal Processing*, vol. 16, pp. 883–917, 8 2022. [Online]. Available: <https://ieeexplore.ieee.org/document/9847080/>
- [37] D. Semmler, M. Joham, and W. Utschick, "High snr analysis of ris-aided mimo broadcast channels," in *2023 IEEE 24th International Workshop on Signal Processing Advances in Wireless Communications (SPAWC)*. IEEE, 9 2023, pp. 221–225. [Online]. Available: <https://ieeexplore.ieee.org/document/10304487/>
- [38] R. Bhatia, "Linear algebra to quantum cohomology: The story of alfred horn's inequalities," *The American Mathematical Monthly*, vol. 108, pp. 289–318, 4 2001. [Online]. Available: <https://www.tandfonline.com/doi/full/10.1080/00029890.2001.11919754>
- [39] L. Hogben, *Handbook of Linear Algebra*. CRC press, 2013.
- [40] G. Bartoli, A. Abrardo, N. Decarli, D. Dardari, and M. D. Renzo, "Spatial multiplexing in near field mimo channels with reconfigurable intelligent surfaces," *IET Signal Processing*, vol. 17, 3 2023. [Online]. Available: <https://ietresearch.onlinelibrary.wiley.com/doi/10.1049/sil2.12195>
- [41] K. Gomadam, V. R. Cadambe, and S. A. Jafar, "A distributed numerical approach to interference alignment and applications to wireless interference networks," *IEEE Transactions on Information Theory*, vol. 57, pp. 3309–3322, 6 2011. [Online]. Available: <http://ieeexplore.ieee.org/document/5773023/>
- [42] B. Clerckx and C. Oestges, *MIMO Wireless Networks: Channels, Techniques and Standards for Multi-Antenna, Multi-User and Multi-Cell Systems*. Elsevier Science, 2013. [Online]. Available: <https://books.google.co.uk/books?id=drEX1J7jHUIC>
- [43] F. Negro, S. P. Shenoy, I. Ghauri, and D. T. Slock, "Weighted sum rate maximization in the mimo interference channel," *IEEE*, 9 2010, pp. 684–689. [Online]. Available: <http://ieeexplore.ieee.org/document/5671658/>